Shallow Turbulence in Rivers and Estuaries

Stefan A. Talke
Civil and Environmental Engineering Department, Portland State University
PO Box 751-CEE
Portland, OR 97207-0751
phone: (503) 725-2870 fax: (530) 725-4282 email: s.a.talke@pdx.edu

Ed Zaron
Civil and Environmental Engineering Department, Portland State University
PO Box 751-CEE
Portland, OR 97207-0751
phone: (503) 725-2435 fax: (530) 725-4282 email: zaron@cecs.pdx.edu

Chris Chickadel
Applied Physics Lab, University of Washington
1013 NE 40th St
Seattle, WA, 98105
phone: (206) 7221-7673 fax: (206) 543-6785 email: chickadel@apl.washington.edu

Award Number: N00014-12-1-0218, N00014-12-1-0219

LONG-TERM GOALS

The overall long-term goal of the “Shallow Turbulence in Rivers and Estuaries" is to gain a better understanding of turbulent mixing processes and energy dissipation in estuaries and rivers. Specifically, the project goals are to improve understanding of the eddying motion occurring at horizontal length scales greater than the water depth. Improved understanding of such “shallow turbulence” will facilitate interpretation and utilization of remotely-sensed signatures as observed in rivers and estuaries, and in the vicinity of inlets and river mouths. Calibration and interpretation of non-eddying hydrodynamic models may also be improved, leading to improved modeling of turbulent transport.

OBJECTIVES

The “Shallow Turbulence in Rivers and Estuaries” project is analyzing and comparing Delft3D numerical data, existing field data and remotely sensed data for evidence of large scale, quasi-2D eddies that are much larger than the depth. Specific objectives are to:

1. *Determine spatial patterns of shallow turbulence from in-situ and remote sensing data and investigate the effects and interactions of these structures with bottom boundary layer processes and turbulence statistics;*

Report Documentation Page

Form Approved
OMB No. 0704-0188

1. REPORT DATE	2. REPORT TYPE	3. DATES COVERED
2012	**N/A**	**-**

4. TITLE AND SUBTITLE	5a. CONTRACT NUMBER
Shallow Turbulence in Rivers and Estuaries	5b. GRANT NUMBER
	5c. PROGRAM ELEMENT NUMBER
6. AUTHOR(S)	5d. PROJECT NUMBER
	5e. TASK NUMBER
	5f. WORK UNIT NUMBER
7. PERFORMING ORGANIZATION NAME(S) AND ADDRESS(ES) **Civil and Environmental Engineering Department, Portland State University PO Box 751-CEE Portland, OR 97207-0751**	8. PERFORMING ORGANIZATION REPORT NUMBER
9. SPONSORING/MONITORING AGENCY NAME(S) AND ADDRESS(ES)	10. SPONSOR/MONITOR'S ACRONYM(S)
	11. SPONSOR/MONITOR'S REPORT NUMBER(S)

12. DISTRIBUTION/AVAILABILITY STATEMENT
Approved for public release, distribution unlimited

13. SUPPLEMENTARY NOTES
The original document contains color images.

14. ABSTRACT

15. SUBJECT TERMS

16. SECURITY CLASSIFICATION OF:			17. LIMITATION OF ABSTRACT	18. NUMBER OF PAGES	19a. NAME OF RESPONSIBLE PERSON
a. REPORT	b. ABSTRACT	c. THIS PAGE			
unclassified	**unclassified**	**unclassified**	**SAR**	**13**	

2. *Elucidate the conditions of shallow turbulence production through a model parameter study, and determine the optimal model configuration that statistically reproduces the shallow turbulence observed from in-situ records; and*
3. *Synthesize and understand the implications of shallow turbulence by means of the turbulent kinetic energy balance, statistical methods, and collapsing data onto a phase diagram.*

APPROACH

Our approach combines (1) numerical modeling and (2) analysis of existing data to study the dynamics and significance of shallow turbulence in rivers and estuaries. The Delft3D modeling system is being used to perform simulations of shallow turbulence in the Columbia River Estuary (CRE), over a domain that extends from the continental shelf to the end of the tidal river at Bonneville Dam. Previously measured infra-red images and surface currents are being analyzed from the Snohomish River, WA (see Chickadel et al., 2011) as well as from six East Coast Rivers (using data from Areté, Associates). In-situ flow data from the Snohomish River (Talke et al., 2012) and "Mega-Transect data" from the Columbia River mouth (Moritz et al., 2005) are being compared to remote sensing data and modeling results, respectively.

Our analysis strategy consists of (a) identifying and characterizing large scale 2D eddies, and (b) analyzing the statistics of turbulence in model results, remote sensing data, and in-situ field data. The simplest method of visualizing eddies involves subtracting out a mean velocity (the so-called Gallilean transform). Vorticity maps also define regions of eddies, but may also simply identify regions of high shear (and no eddies). Zhou et al., 1996, 1999, and Adrian et al, 2000 define 'swirl analysis', which detects an eddy when the eigenvalues of the two-dimensional spatial velocity gradient matrix (velocity gradient tensor) are imaginary. This method has the advantage of not detecting false positives (unlike vorticity estimates in high-shear areas) and being independent of the frame of reference.

We are also evaluating the turbulent kinetic energy budget (TKE). Neglecting cross-stream terms, the change in TKE over time is caused by turbulent flux divergence due to pressure (T_p), turbulent flux divergence due to dispersion (T_d), the production of turbulence (P) and the dissipation of turbulence ε. For field results, the quantity T_d can be estimated using the methods described in Stacey(2003), production P can be estimated using Stacey et al. (1999), and dissipation ε can be calcuated using the inertial cascade method (e.g., Chickadel et al., 2011) or the structure function method (Wiles et al., 2006). For numerical results, the Reynolds stress and triple correlation products needed for P and T_d are more directly calculable.

WORK COMPLETED

In the 6 months since the project began in March 2012, we have made progress in analyzing in-situ data, remotely sensed data, and in modeling the Columbia River estuary. S. Talke has analyzed bottom turbulence processes in the Snohomish and has investigated the effects of water depth on the drag coefficient and shallow turbulence. The observed depth effects (see 'results') are being incorporated into a manuscript submitted by Talke et al., 2012, which is undergoing revision. C. Chickadel has analyzed both intermediate scale (10 m) and river-width scale (100 m) infra-red and velocity signatures. While camera jitter makes interpretation of the 100 m scale results difficult, the 10 m scale

images show promise (see results). With a similar goal of extracting large scale turbulent structures, S. Talke has performed initial analysis on the Areté, Inc. remotely-sensed surface velocity data.

The bathymetry and grid of our Delft3D model has recently been updated by E. Zaron and a student employed by S. Talke to include flood plains, secondary channels, and all large-scale pile dikes between the mouth of the Columbia (km 0) and the end of tidal influence at Bonneville Dam (km 230). Recent flood-plain measurements (LIDAR) and Army-Corps bathymetry from 2005 were used. Pile dikes are modeled using the 'Thin Dams' functionality of Delft3D; these features are necessary to model the correct tidal propagation in the estuary. We have refined the grid at the Columbia inlet and increased the number of vertical layers to 45 (from 20). The model is run with realistic tidal forcing and measured river flow rates from August 2005. To date, we have investigated the sensitivity of shallow turbulence to three parameters: grid spacing, time step, and the Chezy friction coefficient. These results are currently being evaluated and compared to the Mega-Transect data collected by the Army Corps and the tidal inlet. Zaron attended the 3rd International Symposium on Shallow Flows, at the University of Iowa in June 2012, where he presented analysis of the Mega-Transect data (Zaron et al, 2012).

RESULTS

Remote Sensing Analysis– IR surface velocity data: Nested-scale thermal infrared (IR) imagery was gathered during a 2009 field experiment on the Snohomish River from a suite of imaging platforms (spanning millimeters to tens of meters), principally including two barge-mounted cameras and a balloon camera platform (LTAIRS – Lighter-Than-Air InfraRed System). Using IR data from one of the barge mounted cameras (Figure 1) we employed a Particle Image Velocimetry (PIV) technique (Chickadel et al*., 2011*) to estimate the 2D surface velocity over a 6m x 12m area and investigate large-scale horizontal features. An example of the de-meaned snapshot of the IR based PIV surface velocity is shown in Figure 2. Flow is from the top to the bottom of the image, and the mean velocity is ~0.7 m/s. Numerous meter-scale coherent flow features are associated with the surface expression of boils. However, the time series (timestack) of flow (Figure 2) shows an apparent cross-channel pattern of along-channel flow that is not random.

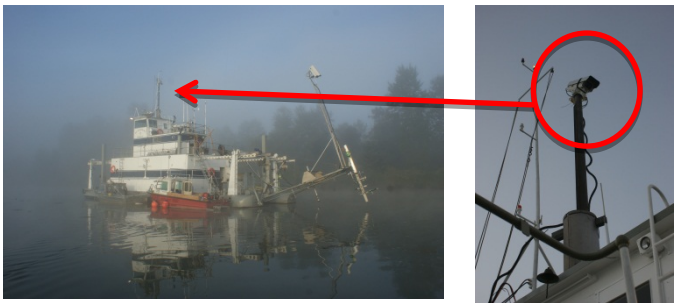

Figure 1. (left) R/V Henderson barge at station in the Snohomish River, WA. (right) A cooled thermal camera mounted on a extendable rotating ram and views the river to the side of the barge.

The cross-channel pattern (boil streets) evident in the timestack corresponds to the preferred surfacing location of boils that could be due to cross-channel variability in boil nucleation points off the bed (3D dunes or bed forms). The bed profile at this location, however, is fairly uniform; instead, secondary circulation (e.g. Nezu et al., *1993*) inherent in open channel flow is a more probable cause. According to Nezu et al. (1993), longitudinal vorticity streets would cause alternating upwelling (boils) and down welling that scales with approximately twice the river depth. The approximately 8 m repetition seen in the surface flow is consistent with the average 4 m depth at this site. Surface flow time series also show a low frequency variability of order 100-200 s (Fig 3). . Figure 3 displays the frequency spectra calculated from each PIV location along the white transect in Figure 2. The mean spectrum (Figure 2) has a specific peak at a period of 159s. Assuming Taylor's frozen turbulence hypothesis, this corresponds to a wavelength of 106m (0.67 m/s mean velocity), which is approximately the same scale as the river width.

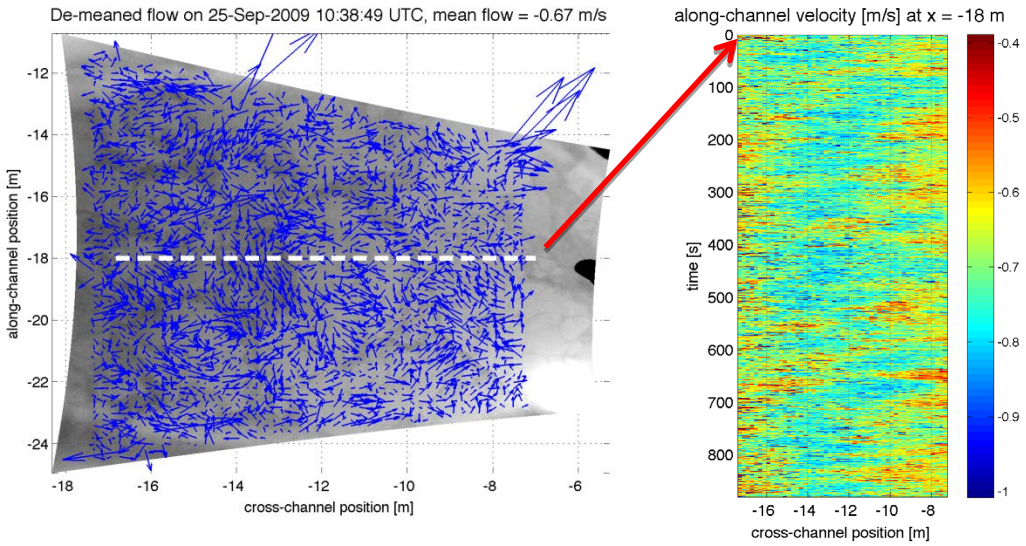

Figure 2. (left) De-meaned surface velocity derived from the IR camera in Figure 1 plotted on a sample IR image from the same time. (right) A 15 minute timestack of along-channel velocities from the transect in the PIV filed indicated by the dashed white line at right. Note the undulating velocity region toward the center of the field of view, which is moving at a faster speed.

Analysis of in-situ ADCP data (nearly) co-located with the IR-video camera also shows a discrete peak in coherence at a frequency of 0.005 Hz (period ~200 seconds) for different vertical lags (Fig. 4). Like the surface measurements, this frequency corresponds to the river width. The coherence of > 0.7 indicates that the motion at ~0.005 Hz penetrates through the entire water column, and suggests that, the width scale motions observed at the surface move as a rigid body throughout the water column. for a probable cause are 2D, river-width horizontal eddies, but we cannot rule out simple instability in the secondary circulation.

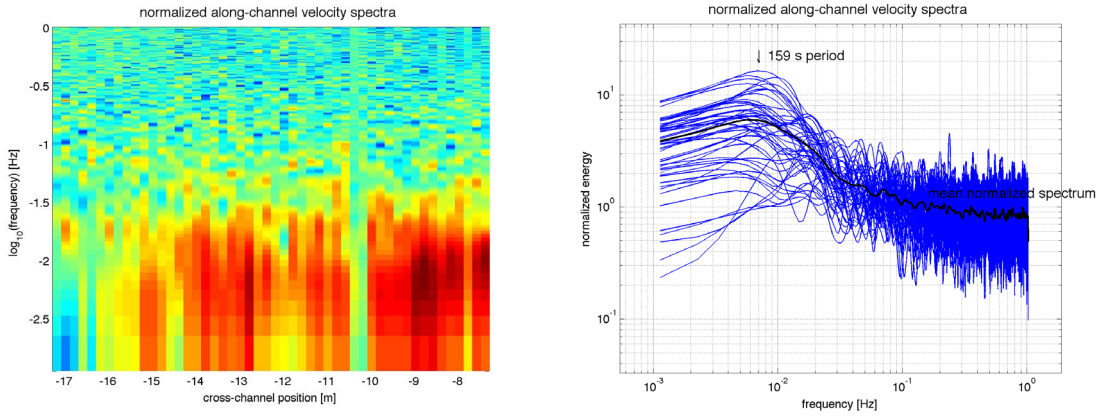

Figure 3. (left) Frequency spectra from the time series in Figure 2 displayed as a color mapped image. (right) Spectra (blue) from each cross-channel location overlaid with the mean spectra indicating a dominant low frequency component with ~160s period.

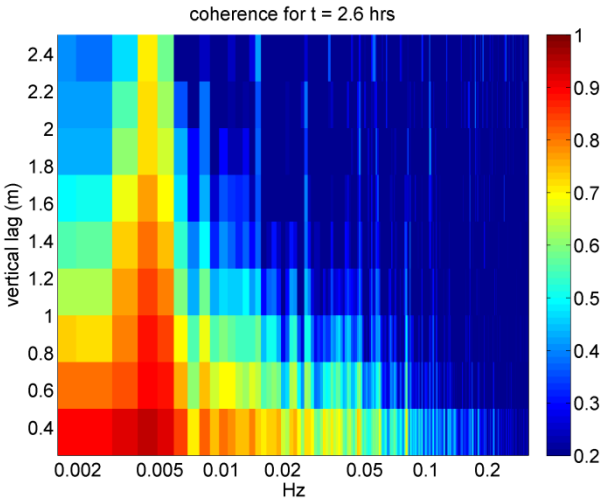

Figure 4: Coherence plot for the in-situ ADCP which was mounted on the barge in the Snohomish River (see Figure 1). Coherence is a normalized co-spectra with a value between zero (uncorrelated) and one (perfectly correlated). The coherence between vertically separated bins of the along-beam velocity were calculated, and averaged for different vertical lags.

To gain understanding of the features observed in the Snohomish River, we are beginning to analyze larger spatial scales using airborne flow data provided by Areté Associates to identify cross-channel coherent motions. Initial analysis shows that ribbons of elevated vorticity are present in surface flows where there is large shear (Fig. 5). The vorticity ribbons or streaks are typically associated with discrete areas containing a significant 'swirling strength'. These areas depict large eddying motion with a length scale of up to half the river width, as shown by the overlaid contours in Fig. 5b. These eddies appear to be primarily attached to the lateral boundaries, and show some evidence of growing with distance downstream. It is an active area of research to determine what sets the length-scale of the laterally-attached eddies, and how these eddies interact with bottom boundary generated turbulence.

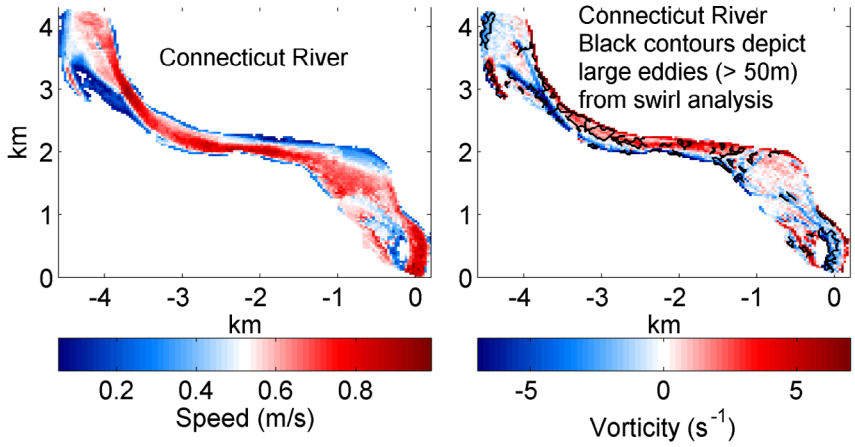

Fig. 5 The flow structure of the Connecticut River, measured in Aug. 2010 by Areté Associates using airborne IR data (left figure). The right hand figure shows the associated vorticity, with areas of significant swirling strength indicated by black contour lines.

In-situ analysis of Snohomish River data: The in-situ analysis since the start of the project in March 2012 has focused on analyzing bottom boundary generated turbulence and its relationship to larger motions that scale with the river width. While this effort is ongoing, we can report a major result that addresses an inconsistency in how numerical models model bottom drag. Figure 6-a shows estimates of the drag coefficient measured over time at a location in the Snohomish River estuary in September 2009. Contrary to the assumption made in many field efforts (Fong et al., 2009; Kim et al., 2000) and most estuarine numerical models (Warner et al., 2005, MacCready et al., 2009; and many others), the drag coefficient varies with time and doubles over the course of an ebb tide from 0.005 to 0.01. Similarly, turbulent statistics such as the along-stream velocity variance (Fig. 6-b) have a large spread when normalized by 'the usual' forcing variables such as u^2. This apparent incongruity with accepted theory is resolved by noting that the spread in Fig. 6-b is reduced by 50% when u'^2 is normalized by $(d/H)\,u^2$, where d/H is the relative ratio of dune height to water depth. Because the drag coefficient is proportional to relative roughness d/H (Fig. 6-a), we find the same result when normalizing u'^2 by $C_d\,u^2$. These observations suggest that the drag coefficient could be parameterized by $C_d \sim (1/H)^a$, where a =1. While the Fig.6 results are inconsistent with the quadratic drag law, more than a century of engineering research suggests that there is in fact a depth dependence to bottom friction, via the empirically derived Manning's law (Dooge, 1992). Using the theoretical derivation in Gioia and

Bombardelli, 2002, we find that the drag coefficient in Manning's law varies with the relative roughness *d/H* as

$$C_d \sim \left(\frac{d}{H}\right)^a \quad , \qquad (1)$$

where a =1/3. While the 1/3 scaling suggested in Eq. 1 is different than the a =1 scaling suggested by Fig. 6, we note that our dynamic range (0.1 < d/H < 0.2) was not enough to determine an accurate coefficient. More research is needed to confirm our findings, and it is possible that a local flow feature is forcing the observed *d/H* dependance. However, our results are consistent with the Manning formulation to first order, rather than the quadratic drag coefficient.

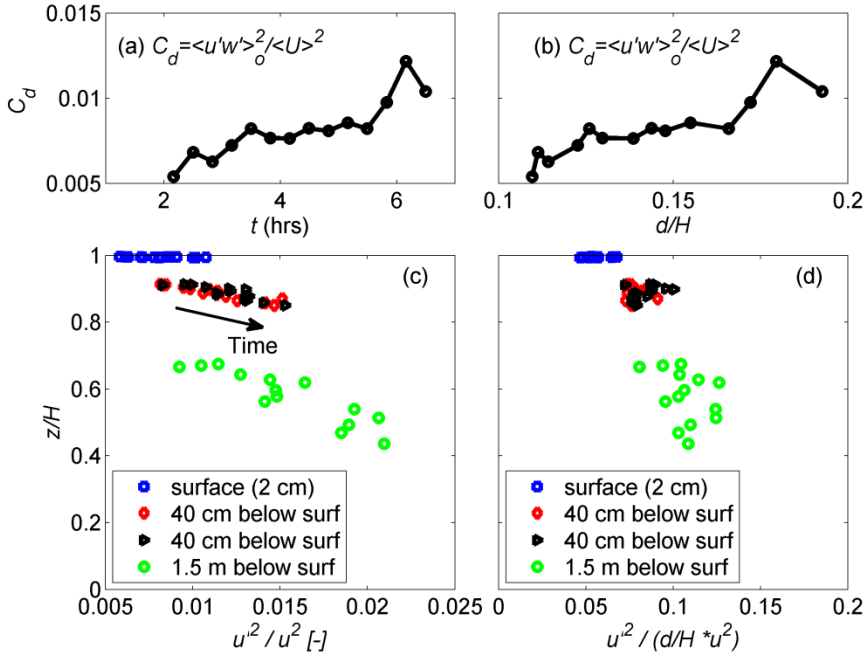

Figure 6 Drag coefficient and along-stream variance (a component of turbulent kinetic energy) from the Snohomish River data set of Sept. 2009. The drag coefficient changes vs. time (a) and is approximatley linearly proportional to the relative roughness d/H, where d = the dune height and H is the water depth (b). The along-stream velocity variance shows more spread when normalized by u^2 (c) than by d/H $u^2 \sim C_d u^2$ (d).

Other statistics such as TKE dissipation cooberate the interpretation that the drag coefficient is inversely related to water depth.; dissipation statistics, for example, show a 50% decrease in spread when normalized by d/H $*U^{3}/H$ rather than simply the canonical U^{3}/H (Fig. 7). A depth-dependent drag-coefficient likely impacts shallow turbulence through the so-called 'shear stability number', $S = \frac{\varepsilon_{BBL}}{\varepsilon_{nD}} = \frac{WC_d}{H}$, which is defined as the ratio between bottom boundary generated dissipation and dissipation generated from quasi-2D, large aspect ratio eddies with width W. At the Snohomish River field site, the drag-dependent shear stability parameter varies from 0.1 (early ebb) to 0.4 (late ebb), which suggests that BBL processes are becoming more important. We are currently investigating whether any tangible (in-situ or remote) changes are observed as the shear-stability parameter varies.

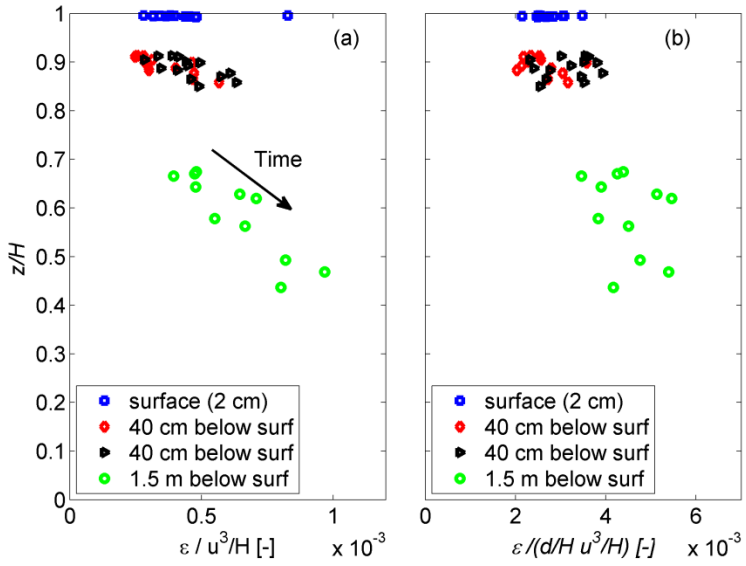

Figure 7: Energy dissipation normalized by U^3/H (a) and by $d/H\ U^3/H \sim C_d\ U^3/H$ (b). Larger spread is observed in (a). A hysteresis in time is notated in (a) by an arrow; the total elapsed time in data set is approximately 5 hours.

Delft3D Modeling results and comparison with in-situ data: Initial Delft3D modeling results suggest that modelled shallow turbulence varies with grid structure, vertical resolution, and the bottom friction coefficient. The most dramatic differences occur between unstratified conditions (Fig. 8) and stratified conditions (Fig. 9). Qualitatively, introducing stratification is akin to greatly reducing the effective drag felt by horizontal eddies; hence, we interpret Fig. 8 and Fig. 9 to be extreme cases along a continuum of effects. When there is no stratification, vorticies tend to form and detach from topographic features as discrete eddies, such as is visible south of the South Jetty in Fig. 8. Some vorticity ribbons are also visible.

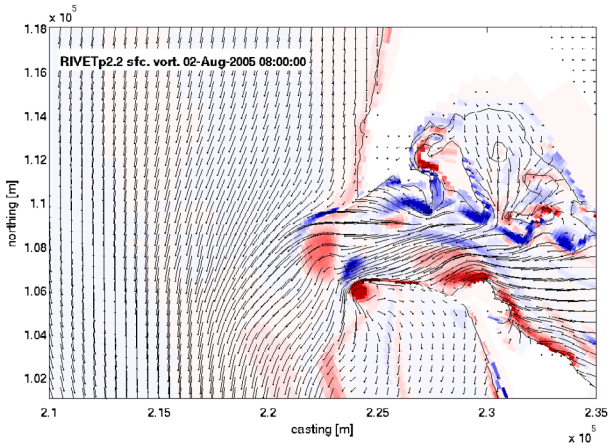

Figure 8: Vorticity at the mouth of the Columbia River during unstratified conditions, with instantaneous streamlines overlaid. Peak vorticity is +/- 0.002 s^{-1}.

By contrast, during stratified conditions the surface flow is marked primarily by vorticity streaks (Fig. 9), and few discrete areas of eddying motion are observed (except in the shallow water of 'Baker Bay' in upper right). Stratification and tidal forcing leads to a system of strong spatial salinity gradients (Fig. 10), which implies that some regions of large vorticity are due to velocity gradients at fronts, rather than eddying motion. Overall, the vorticity ribbons in the tidal inlet and estuary resemble those observed in the Arete data from the Conneticut River (Fig. 5). Therefore, we surmise that some streaks of vorticity in Fig. 8 and Fig. 9 may contain a 'street' of eddies. We plan on applying the 'swirling-strength' analysis to the Delft3D data in the near future to confirm this interpretation.

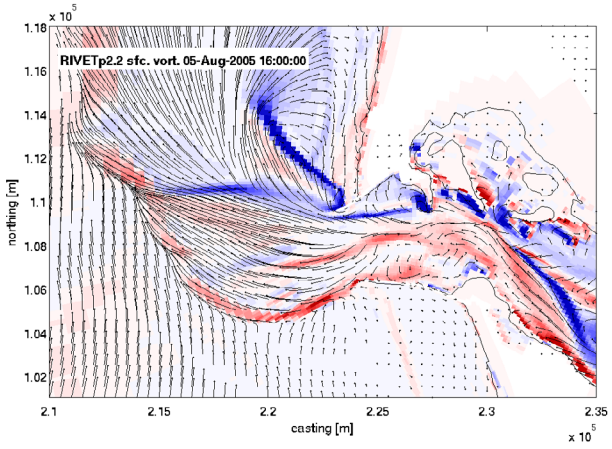

Figure 9: Vorticity at the mouth of the Columbia River during stratified conditions, with instantaneous streamlines overlaid. Peak vorticity is +/- 0.002 s^{-1}

One of our ultimate goals is to determine whether Figs 8-10 are realistic representations of estuary and tidal inlet physics. Comparisons between the Army-Corps Mega-Transect data (located approximately at the coordinate $2.26*10^5$ m easting, $1.08*10^5$ m northing in Figs. 8-10) and the Delft3D data are shown in Fig. 11. To first order the plots look qualitatively similar, although there are differences in the shape of the mean and tidal velocity structure (particularly near the bed). The rms eddy velocity of ~ 20 cm/s in the Army-Corps data is larger than the 10-15 cm/s in the Delft3D results. Interestingly, the eddy structure in both the model and the in-situ results are similar, and suggests that shallow turbulence eddies, as also suggested in Fig. 4, are fairly homogenous throughout the water column. Future work will focus on examining and improving the agreement between the model and the in-situ data by investigating a larger parameter range (e.g., bottom friction, grid size, etc) and through continued dynamical analyses.

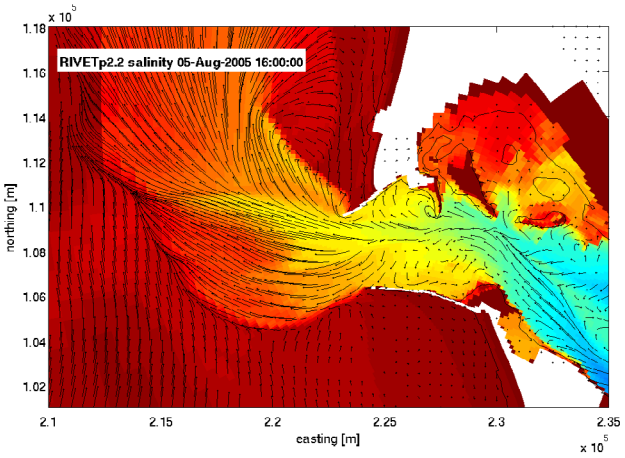

Figure 10: Surface salinity and streamlines observed during the stratified conditions depicted in Fig. 9.

IMPACT/APPLICATIONS

The observation that drag coefficient in the Snohomish River depends on the relative roughness ratio and may be more properly modelled by a Manning-Law than the quadratic drag law is potentially quite important for correctly modelling shallow water estuaries and rivers. In model domains with areas subject to large depth variations (e.g., intertidal areas), the modelled flow will be quantitatively different and potentially incorrect if a quadratic drag law is used.

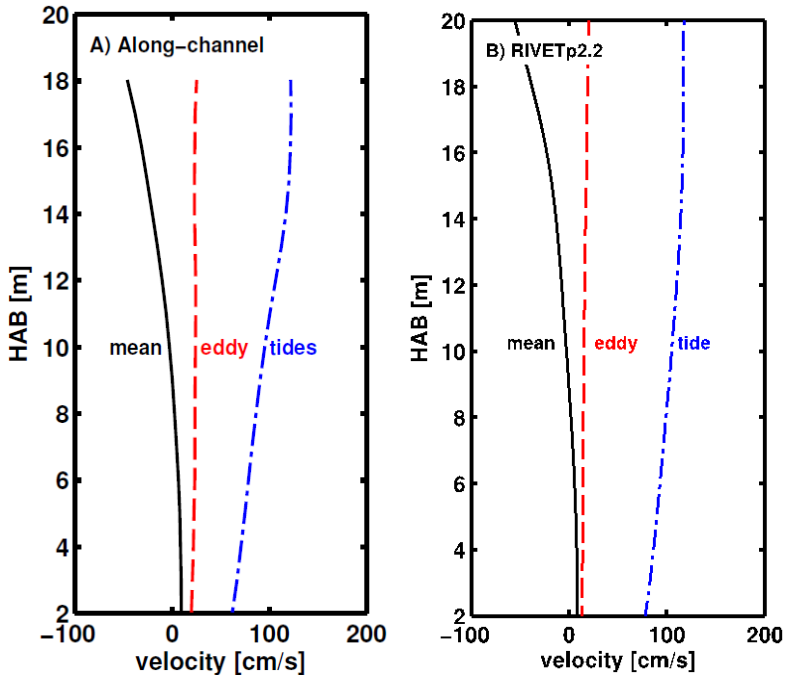

Figure 11. Comparison of the vertical structure of along-stream tidal velocity structure (blue), tidally averaged structure (black) and eddy structure (red) from Army-Corps Mega-Transect data (A-left) and Delft3D model run (B-right).

The work on understanding shallow turbulence and its surface signatures in remotely sensed data potentially provides tools for understanding complex environments and constraining/optimizing models. The degree of surface vorticity provides direct evidence of the effect of bottom boundary processes; when frictional effects are small or stratification large, surface currents organize in vorticity ribbons that contain large eddying motion or 'shallow turbulence'. By contrast, strong mixing tends to make 'shallow turbulence' signatures more discrete and tied to topagraphy. Hence, the characteristics of surface vorticity likely provides an indication of the underlying friction and stratification, which can be used to calibrate/interpret models and remotely sensed data.

RELATED PROJECTS

There are no current related projects

REFERENCES

Adrian, R.J., K.T. Christensen, Z.-C.Liu, (2000). Analysis and interpretation of instantaneous turbulent velocity fields, *Experiments in Fluids* **29**, 275-290.

Anderson & Dugan, (2011). Surface Currents in Rivers and Estuaries derived from airborne IR remote sensing, Areté Associates pdf.

Chickadel, C. C., Talke, S. A., Horner-Devine, A. R., and Jessup, A. T. (2011). Infrared-based measurements of velocity, turbulent kinetic energy, and dissipation at the water surface in a tidal river. *Geoscience and Remote Sensing Letters, ,* GRSL-00530-2010.R1

Dooge, J. C. I., in *Channel Wall Resistance: Centennial of Manning's Formula,* edited by B. C. Yen

Dugan, J. P. and Piotrowski, C. C. (2011). EO observations of currents and turbulence via mixing of sediment load variations. In *IEEE/OES 10th Current, Waves and Turbulence Measurement Conference* (CWTMC '11), Monterey, CA. IEEE.

Fong, D.A., S.G. Monismith, J.R. Burau, and M.T. Stacey, "Observations of secondary circulation and bottom stress in a channel with significant curvatures," J. ASCE Hydr. Div. 135(3), pp. 198-208, 2009

Gioia, G., & F.A. Bombardelli, 2002. Scaling and Similarity in Rough Channel Flows, *Physical Review Letters*, Vol. 88(1).

Kim, S.C., C.T. Friedrichs, J.P.Y. Maa, & L.D. Wright, 2000, *Estimating Bottom Stress in Tidal Boundary Layer from Acoustic Doppler Velocimeter Data. Journal of Hydraulic Engineering., June 2000, p. 399-406*

MacCready, P., N.S. Banas, B. M.Hickey, E. P. Dever, Y. Liu, 2009. A model study of tide and wind-induced mixing in the Columbia River Estuary and plume, *Continental Shelf Research,*p. 278-291.

Moritz, H. R., Gelfenbaum, G. R., and Ruggiero, P. (2005). Morphological implications of oceanographic measurements acquired along a mega-transect at the mouth of the Columbia River, USA. In *American Geophysical Union, Fall Meeting, pages OS23A–1534*. American Geophysical Union.

Nezu, I., Tominaga, A., and Nakagawa, H. (1993). Field measurements of secondary currents in straight rivers. *Journal of Hydraulic Engineering*, 119(5):598–614.

Stacey, M.T., S.G Monismith, & J.R. Burau, (1999). Measurements of Reynolds stress profiles in unstratified tidal flow, *Journal of Geophysical Research-Oceans* **104** (C5), 10933-10949.

Stacey, Mark T. (2003). Estimation of Diffusive Transport of Turbulent Kinetic Energy from Acoustic Doppler Current Profiler Data. *J. Atmos. Oceanic Technol.*, **20**, 927–935. doi: 10.1175/1520-0426(2003)020<0927:EODTOT>2.0.CO;2

Talke, S.A., A.R. Horner-Devine, C.C. Chickadel, and A. T. Jessup,(2012), *in review.* Turbulent kinetic energy and coherent structures in a tidal river Part I: water column turbulence. *submitted to Journal of Geophysical Research.*

Talke, S.A., A.R. Horner-Devine, C.C. Chickadel, and A. T. Jessup, (2012)b *in review.* Turbulent kinetic energy and coherent structures in a tidal river Part II: near surface turbulence. *submitted to Journal of Geophysical Research.*

Warner, J.C., Geyer, W.R., Lerczak, J.A. (2005). Numerical modeling of an estuary: a comprehensive skill assessment. *Journal of Geophysical Research* C5, 2004JC002666.

Wiles, P. J., T. P. Rippeth, J. H. Simpson, and P. J. Hendricks (2006). A novel technique for measuring the rate of turbulent dissipation in the marine environment, *Geophys. Res. Lett.*, 33, L21608, doi:10.1029/2006GL027050.

Zhou, H., R.J. Adrian, S. Balachandar (1996). Autogeneration of near wall vertical structures in channel flow. *Physics of Fluids* 8: 288-290.

Zaron, E.D., H.R. Moritz, and G.R. Gelfenbaum (2012). Characteristics of Shallow Turbulence in the Mouth of the Columbia River, talk presented at the 3rd International Symposium on Shallow Flows, University of Iowa, Iowa City, June 4-6.

PUBLICATIONS

Talke, S.A., A.R. Horner-Devine, C.C. Chickadel, and A. T. Jessup,(2012), *in review.* Turbulent kinetic energy and coherent structures in a tidal river Part I: water column turbulence. *submitted to Journal of Geophysical Research.*

Zaron, E.D., H.R. Moritz, and G.R. Gelfenbaum (2012). Characteristics of Shallow Turbulence in the Mouth of the Columbia River, talk presented at the 3rd International Symposium on Shallow Flows, University of Iowa, Iowa City, June 4-6.

HONORS/AWARDS/PRIZES

ONR Young Investigator Program: Stefan Talke, Civil and Environmental Engineering, Portland State University